Photonics applications IV

- ✓ Fabrication of GhG optical fiber
- ✓ Fabrication of ChG planar waveguide
- ✓ Fabrication of ChG PC structure

Why does fabrication issue matter for photonics applications?

- ✓ Geometrical shape and refractive index difference determine the optical confinements;
  - ➢ Single-mode or multi-mode?
  - ➢ Cross-section of waveguide; circular or rectangular?
- ✓ Loss coefficient is as critical as gain coefficient;
  - ➢ Absorption loss, scattering loss, bending loss…
- ✓ Controlling refractive index profile of a waveguide can manage propagation properties;
  - ➢ Control dispersion properties
  - ➢ Photonic crystals
  - ➢ Phase matching condition in nonlinear applications
  - ➢ Optical splicing between other waveguides; mode-size mismatch and Fresnel reflection

Fiberization of ChG

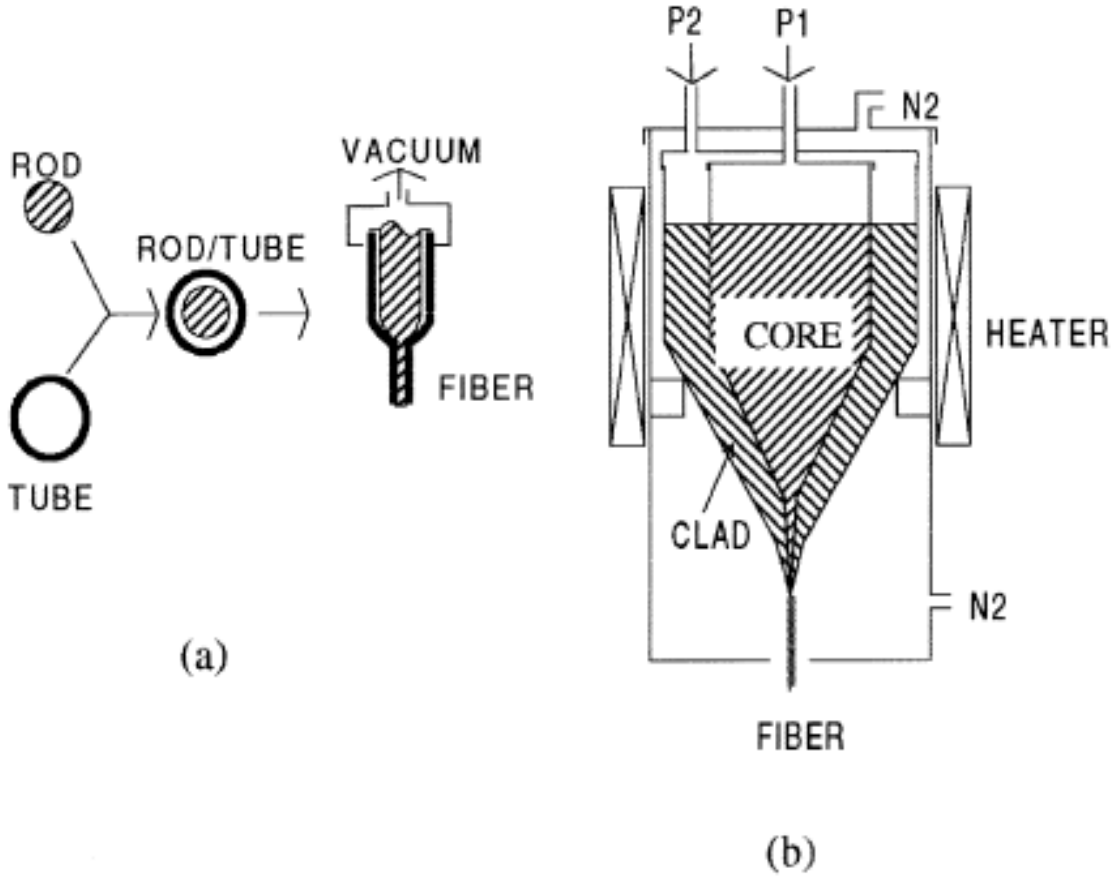

Fig. 1. Schematic representation of fiberization using: (a) rod-in-tube technique and (b) double crucible process (DCP).

Sanghera and Aggarwal, J. Non-Cryst. Solids 256&257 (1999) 6.

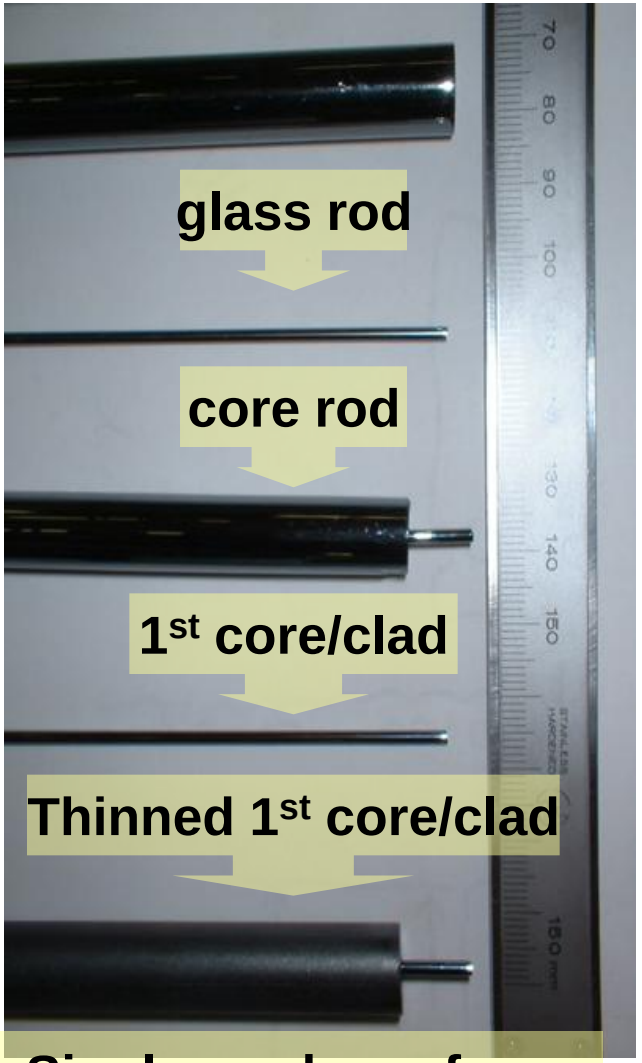

Choi et al, unpublished result

Table 1
Some physical, mechanical and optical properties of chalcogenide glasses used for making optical fibers [17]

	$As_{40}S_{60}$	$Ge_{30}As_{10}Se_{30}Te_{30}$
Physical properties		
T_g (°C)[a]	197	265
CTE (10^{-6} °C)[b]	21.4	14.4
Thermal conductivity (W/m °C)	0.17	~0.2
Mechanical properties		
Density (g/cm^3)	3.20	4.88
Knoop hardness (kg/mm^2)	109	205
Fracture toughness (MPa m$^{1/2}$)	~0.2	~0.2
Poisson's ratio	0.24	~0.26
Youngs modulus (GPa)	16.0	21.9
Optical properties		
Refractive index[c]	2.415 (3.0)	2.80 (10.6)
dn/dT (10^{-5} °C^{-1})[c,d]	+0.9 (5.4)	+10.0 (10.6)
Bulk transmission (μm)	0.6–10.0	1.0–17.0
Fiber transmission (μm)	0.8–6.5	3.0–11.0
Lowest loss (dB/km)[c]	23 (2.3)	110 (6.6)
Typical loss (dB/km)[c]	100–200 (2.2–5.0)	500–1000 (6.0–9.0)
Estimated minimum loss (dB/km)[c]	1.0	n.d.

[a] T_g is the glass transition temperature.
[b] CTE is the coefficient of thermal expansion.
[c] Wavelength in μm given in parenthesis.
[d] dn/dT is the change in refractive index with temperature.
n.d. – not determined.

Sanghera and Aggarwal, J. Non-Cryst. Solids 256&257 (1999) 6.

Attenuation

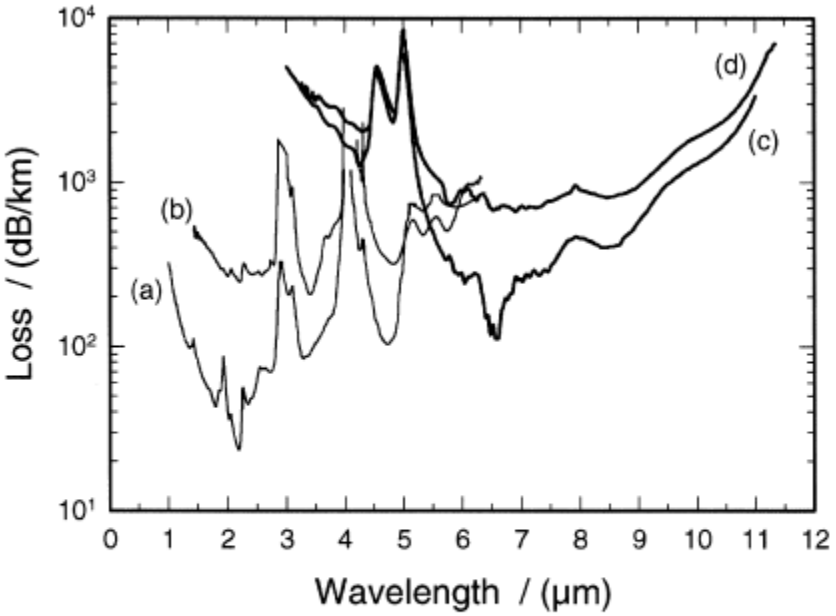

Fig. 3. Transmission loss (± 10 dB/km) spectra of (a) lowest loss sulphide fiber, (b) typical sulphide fiber, (c) lowest loss telluride fiber, and (d) typical telluride fiber.

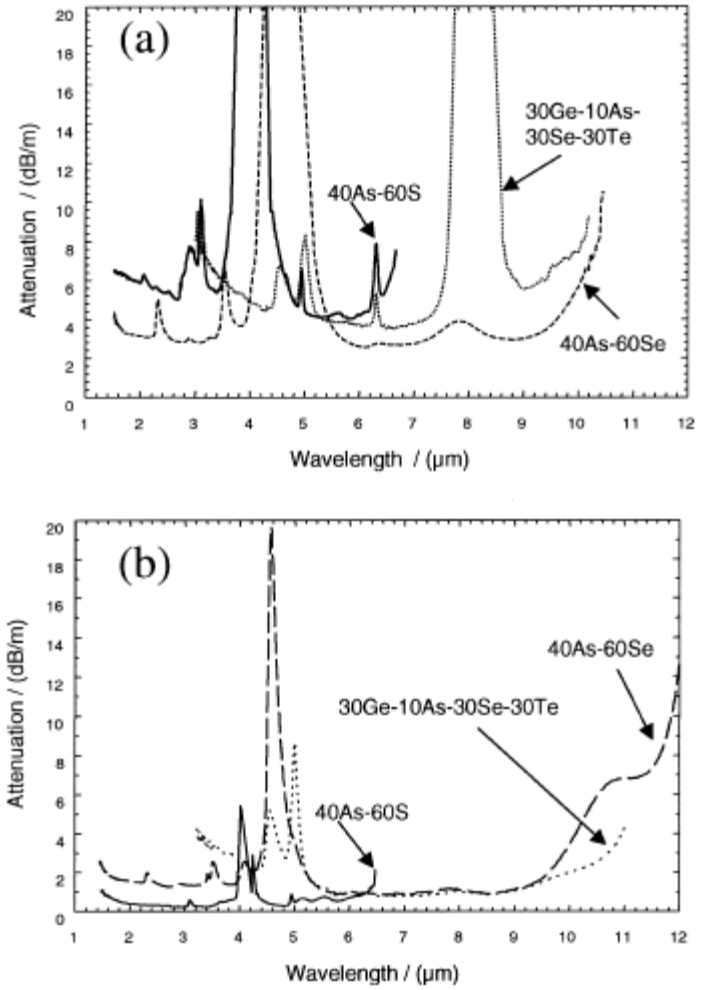

Fig. 2. Transmission loss (±0.01 dB/m) spectra of chalcogenide glass fibers: (a) without purification of chemicals and (b) after purification of chemicals.

Sanghera and Aggarwal, J. Non-Cryst. Solids 256&257 (1999) 6.

Attenuation; silica optical fiber

✓ Perfectly OH-free SMF is commercially available.

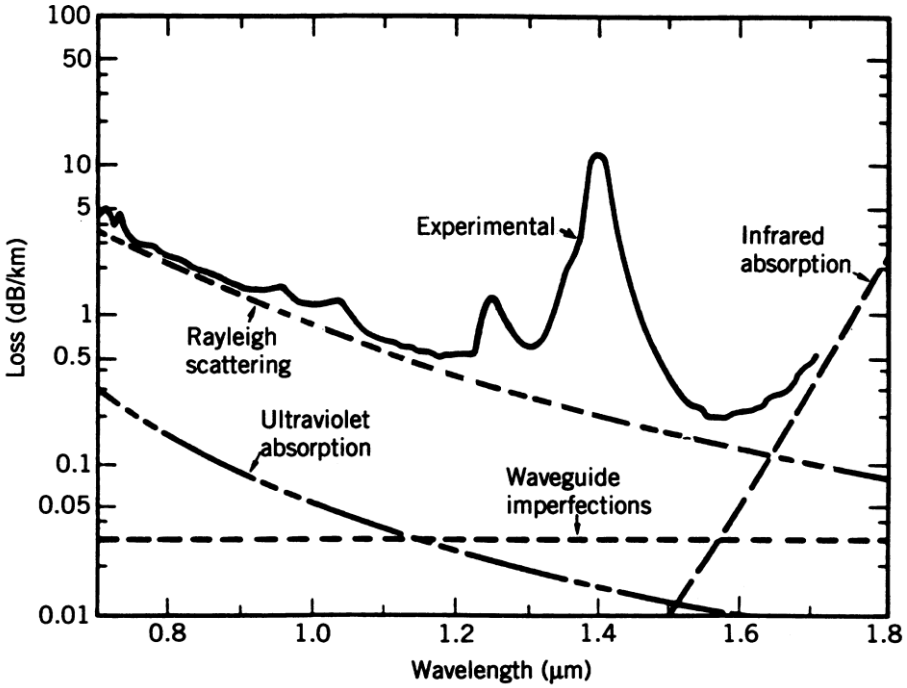

$$\alpha_T = Ae^{a/\lambda} + Be^{-b/\lambda} + \frac{C}{\lambda^4} + D(\lambda) + E(\lambda)$$

A : multiphonon absorption coefficient
B : intrinsic electron absorption coefficient
C : Rayleigh scattering coefficient
D : extrinsic electronic absorption coefficient (ions)
E : extrinsic vibrational absorption coefficient (OH^-)

- Important

Attenuation

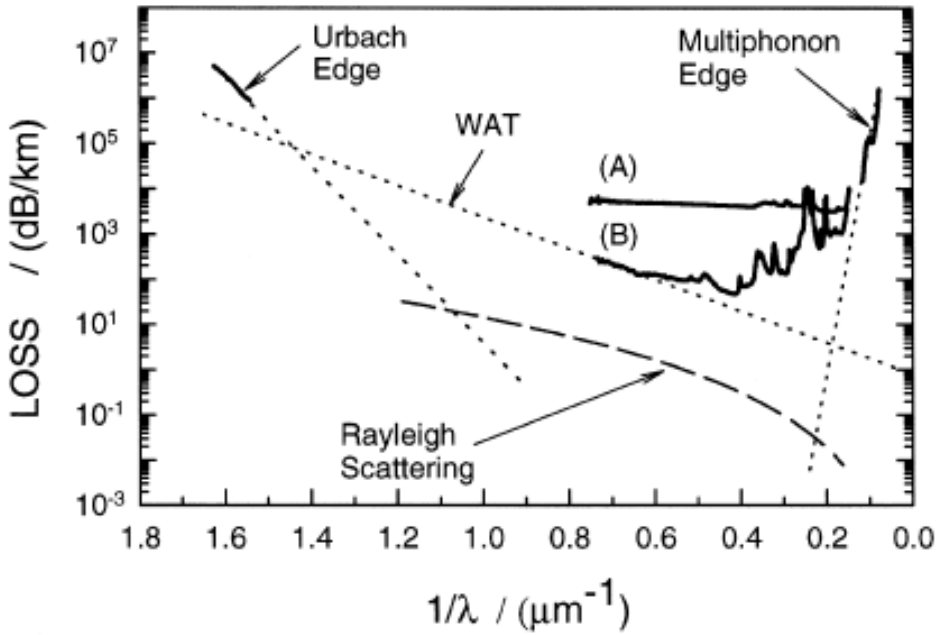

Fig. 4. Estimation of theoretical minimum loss in a sulfide fiber. A and B represent poor and high quality glasses, respectively

Table 2
Estimated concentration of typical impurities in sulphide and telluride fibers [16]

Impurity absorption	Wavelength (μm)	Absorption loss (dB/m)	Extinction coefficient (dB/m ppm)	Impurity concentration (ppm)
Sulfide fibers				
H–S	4.0	10	2.3	4.3
O–H	2.9	0.3	5.0	0.06
Telluride fibers				
H–Se	4.5	3.0	1.1	2.7
Ge–H	5.0	6.0	–	–
H_2O	6.3	0.07	34.0	0.002
Ge–O	7.9	0.16	2.6	0.06

Sanghera and Aggarwal, J. Non-Cryst. Solids 256&257 (1999) 6.

Specialty fiber based on ChG

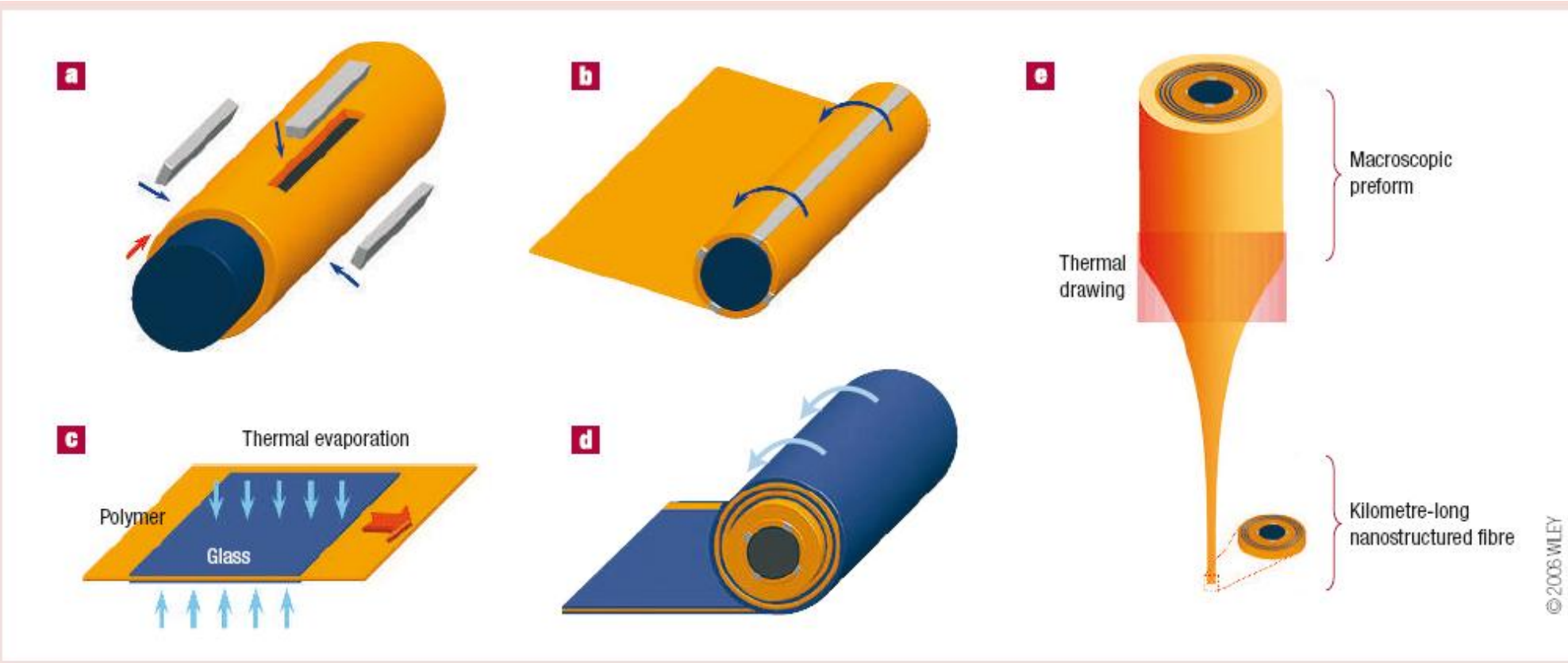

Figure B1 Preform-based fabrication of integrated fibre devices. **a**, A chalcogenide semiconducting glass rod is assembled with an insulating polymer shell and four metal electrodes; and **b**, a polymer sheet is rolled around the structure to form a protective cladding. **c**, The high-index chalcogenide glass is evaporated on both sides of a low-index thin polymer film before **d**, being rolled around the cylinder prepared in **a**,**b**. A polymer layer is wrapped around the coated film for protection. **e**, The preform is consolidated in a vacuum oven and is thermally drawn to mesoscopic-scale fibres. The cross-section of the resulting fibres retains the same structure and relative sizes of the components at the preform level. Reprinted with permission from ref. 28.

Abouraddy et al, Nature Materials 6 (2007) 336.

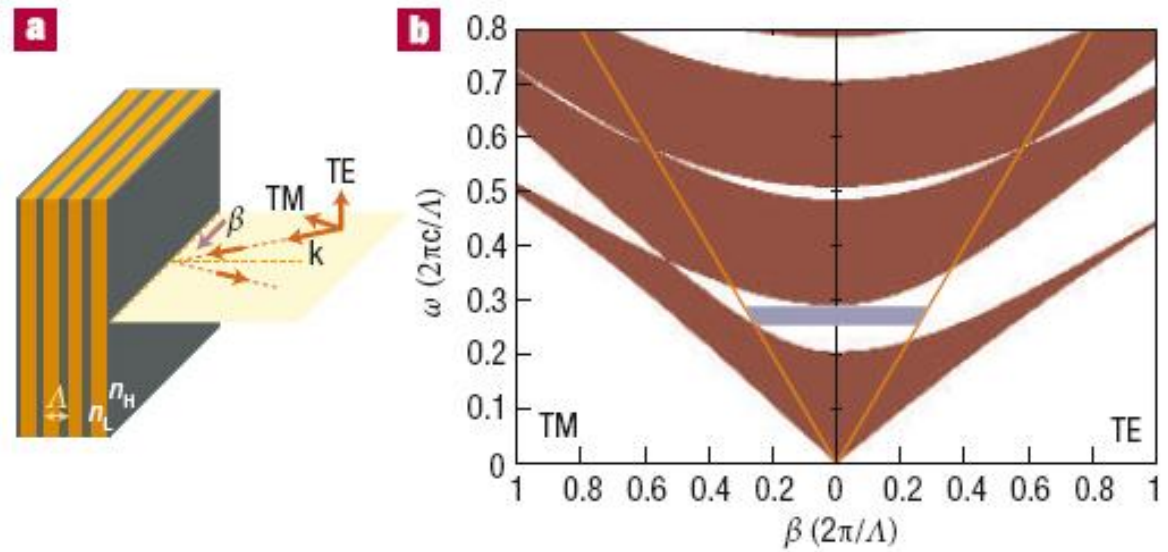

Omnidirectional reflection and light guidance

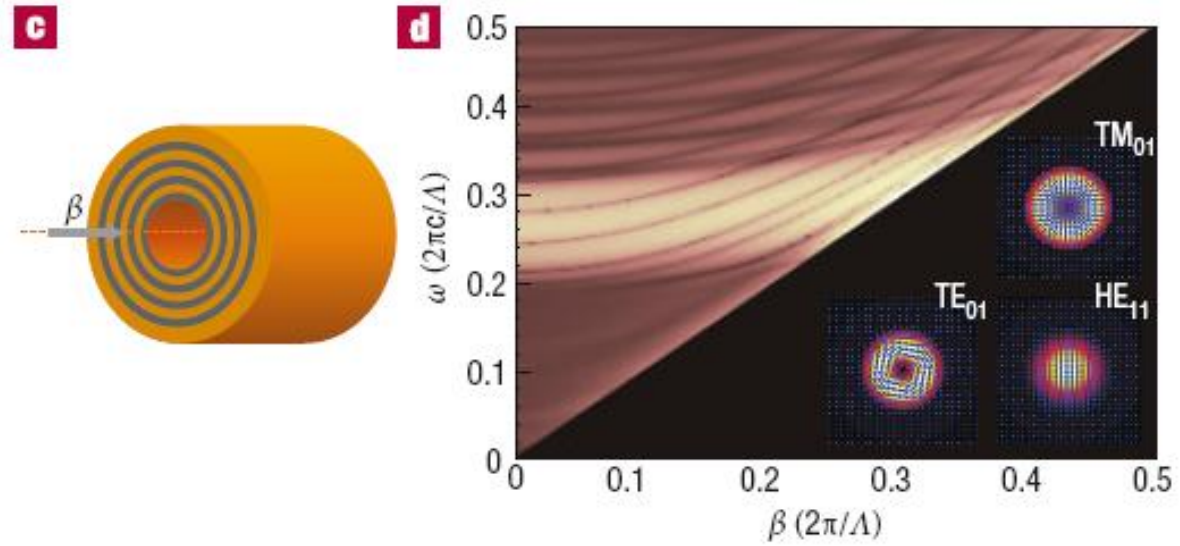

Abouraddy et al, Nature Materials 6 (2007) 336.

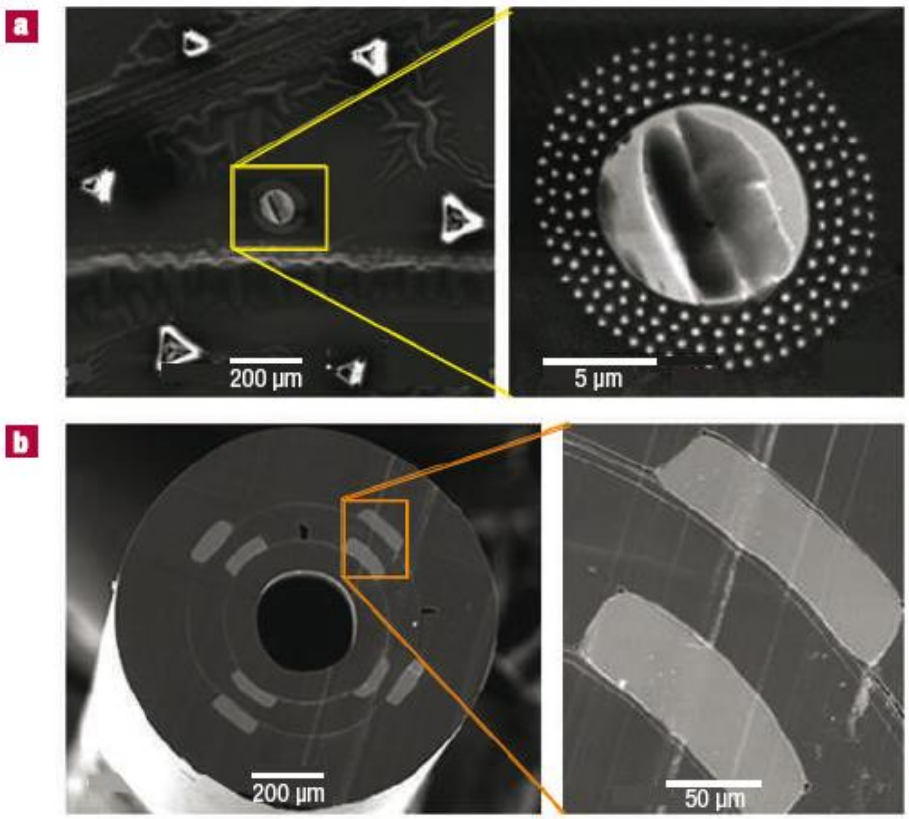

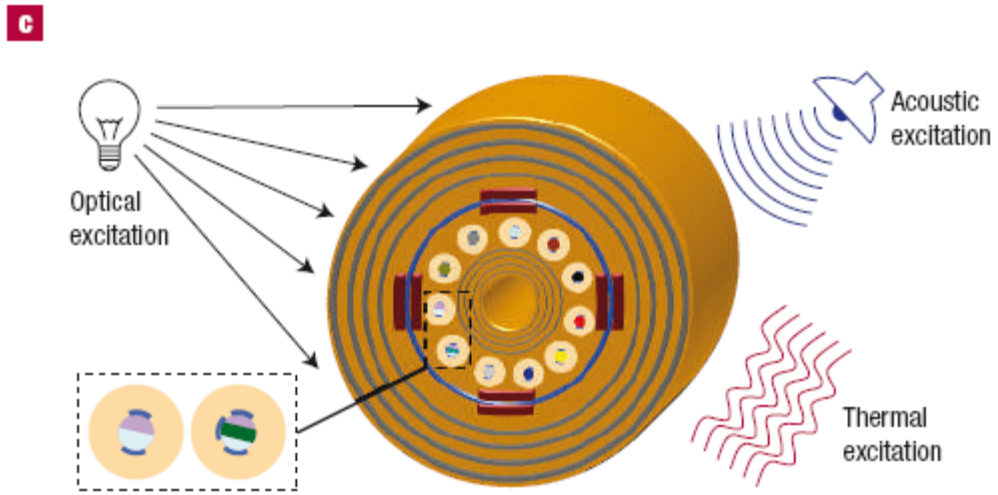

Figure 8 Fibre-device integrated bundles produced by stacking and redrawing. **a**, An array of chalcogenide-glass nanowires surrounding a solid-core of highly nonlinear chalcogenide glass. **b**, Two concentric thin-semiconductor-film devices integrated into the same fibre. **c**, Future vision of integrated fibre-device bundles. A single fibre consists of a hollow core lined with an omnidirectional reflector for optical-power transmission. The fibre is surrounded with another omnidirectional reflector, which may contain multiple cavities, for spectral filtering of externally incident radiation. The fibre contains thin-film semiconducting devices, and also multiple devices distributed over the cross-section, with each device sensitive to a different environmental parameter (light, heat, acoustic waves and so on). Logical operations may also be implemented with simple semiconductor junctions, two of which are shown in the inset.

Abouraddy et al, Nature Materials 6 (2007) 336.

Planar waveguide

- ✓ The smallest nanowires produced in Ge-As-Se
  - ➢ Mode area: ~0.20 μm^2 at 1550 nm
  - ➢ Attenuation loss: ~1.5 dB/cm
  - ➢ Suitable for nonlinear applications due to strong optical confinement
- ✓ For larger waveguides for example*
  - ➢ As_2S_3 rib waveguide with mode areas of 5.7μm^2 and optical losses around 0.05dB/cm at 1550nm
  - ➢ Comparable with the lowest losses achieved in silica planar waveguides
- ✓ Needs of low-loss waveguide for Mid IR applications
  - ➢ Sensing in the molecular fingerprint region between 2 and 20 μm
  - ➢ The commercialization of quantum cascade lasers
  - ➢ Waveguides for the mid-IR with losses as low as 0.5 dB/cm at 8.4 μm

* Gai et al, Optics Express 18 (2010) 26635.

- ✓ Laser patterning
  - ➢ Ge-As-Se-Te glass
  - ➢ Using Ti: sapphire laser

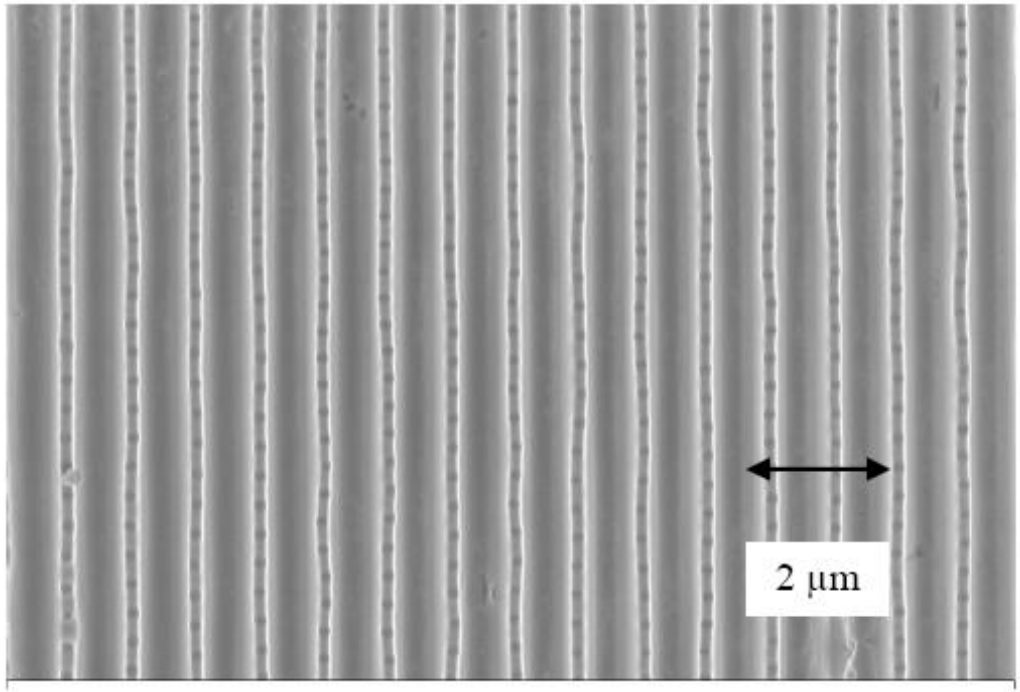

Relief patterns on the surface of Ge-As-Se-Te glass consisting of air grooves (wide dark parallel lines) and glass ribs (bright parallel lines) perforated by air holes (small dark spots).

Paivasaari et al, Opt. Express 15 (2007) 2336.

✓ Photolithography

- ➢ As-S film fabricated via PLD

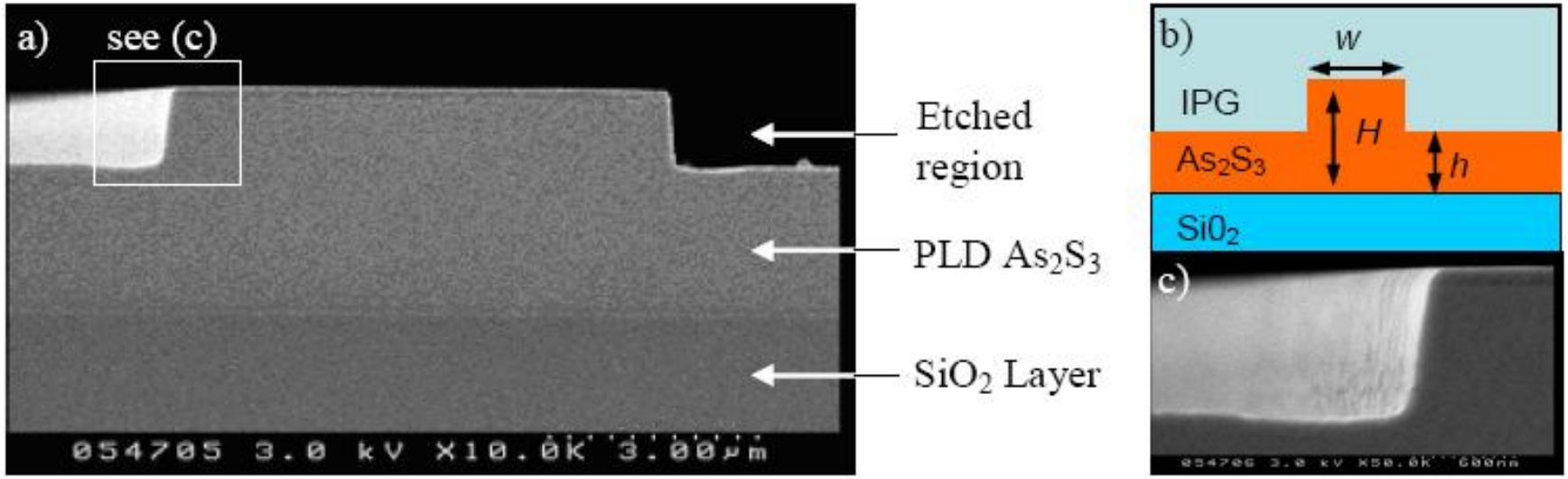

(a) SEM image of a rib-waveguide, (b) schematics of a rib-waveguide structure, and (c) enlarged image from (a) showing minimal sidewall roughness.

Baker, et al, Opt. Express 15 (2007) 1277.

- ✓ Focused ion beam milling using Ga^+ ion beam*
  - ➢ Ge-As-Se film fabricated via PLD
  - ➢ Fabricating 2D PC structure
- ✓ Wet etching + photo-darkening**
  - ➢ As-Se film fabricated via thermal evaporation
  - ➢ Selective etching induced by UV irradiation

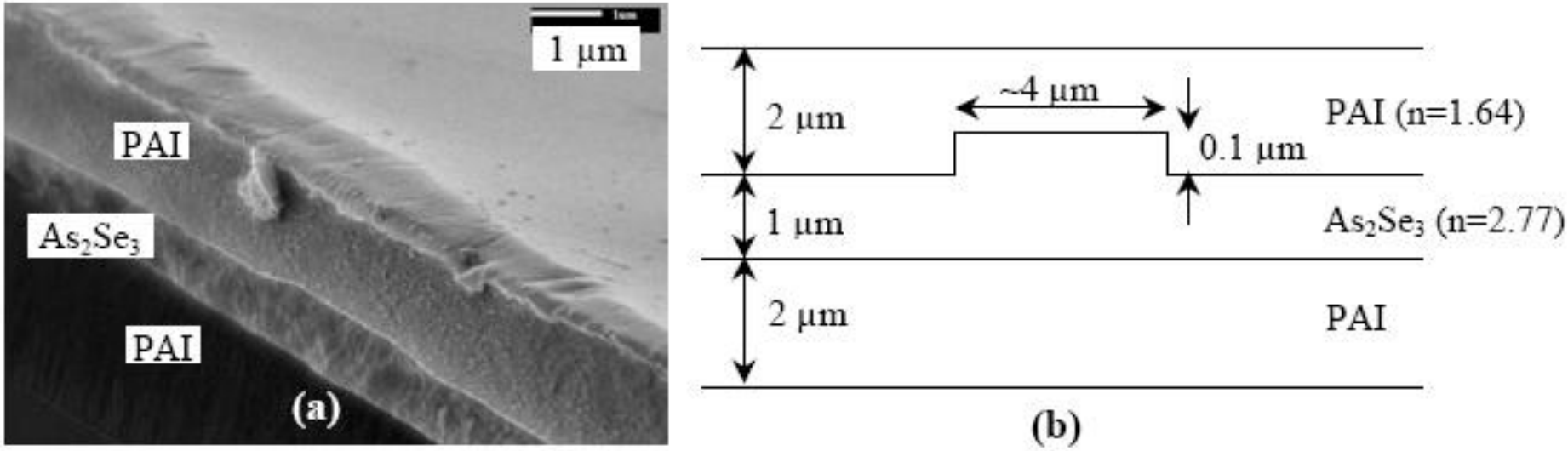

(a) SEM image of the cleaved facet of a rib waveguide and (b) schematic illustration of the rib geometry assumed for simulations.

* Freeman, et al, Opt. Express 13 (2005) 3079.
** Ponnampalam, et al, Opt. Express 12 (2004) 6270.

- ✓ Dry etching (ICP etching)
  - ➢ Various ChG films fabricated via PLD

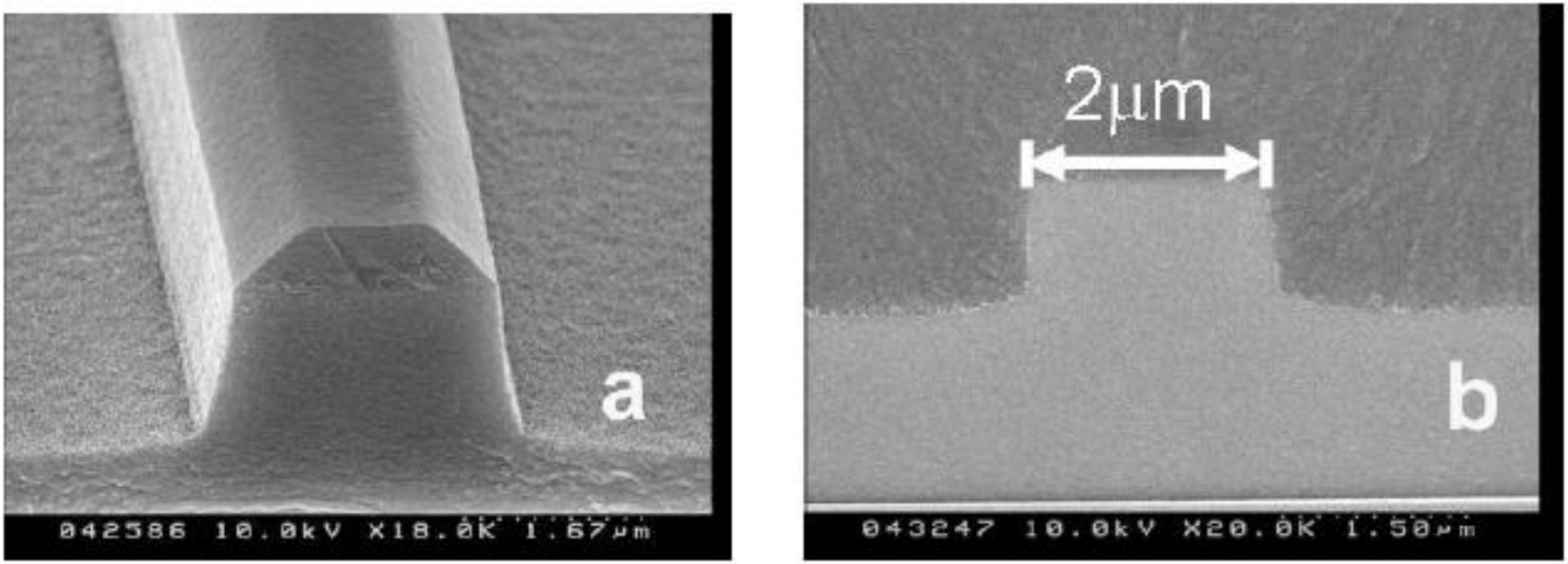

SEM images showing the profile of As-S waveguides etched by ICP using photoresist mask; (a) As-S waveguide with photoresist mask and (b) coating with polymer cladding.

Ruan, et al, Opt. Express 12 (2004) 5140.

- ✓ Hot embossing
  - As-S-Se film
  - Rayleigh scattering limited loss

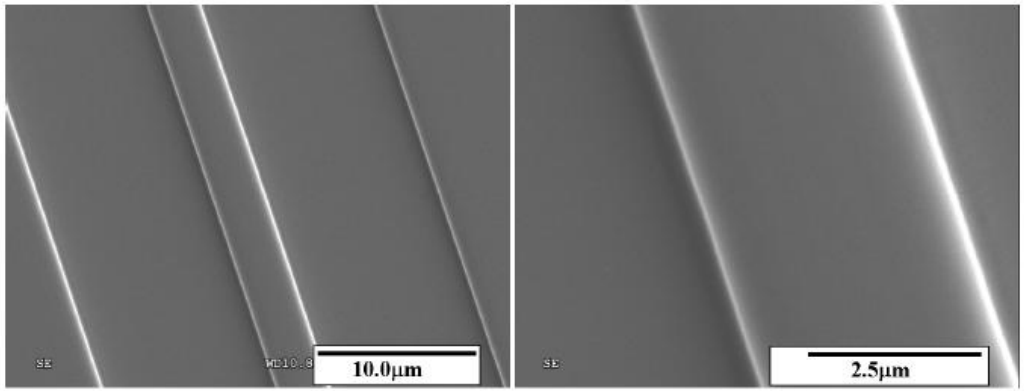

Fig. 2. SEM images of imprinted rib waveguide in $As_{24}Se_{38}S_{38}$ Chalcogenide glass.

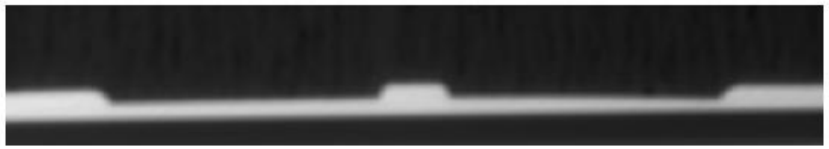

Fig. 3. Cross sectional optical microscope view of the finished imprinted rib waveguide.

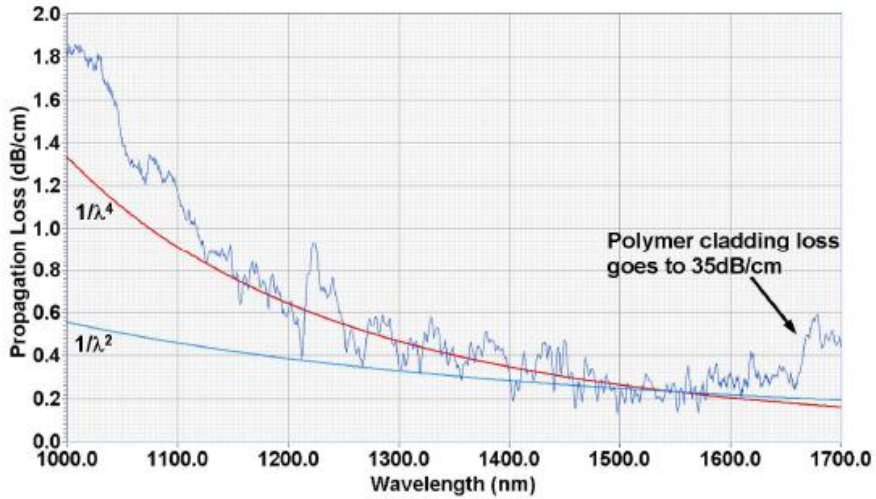

Fig. 5. Measured Optical propagation loss spectrum of 3.3µm wide waveguide.

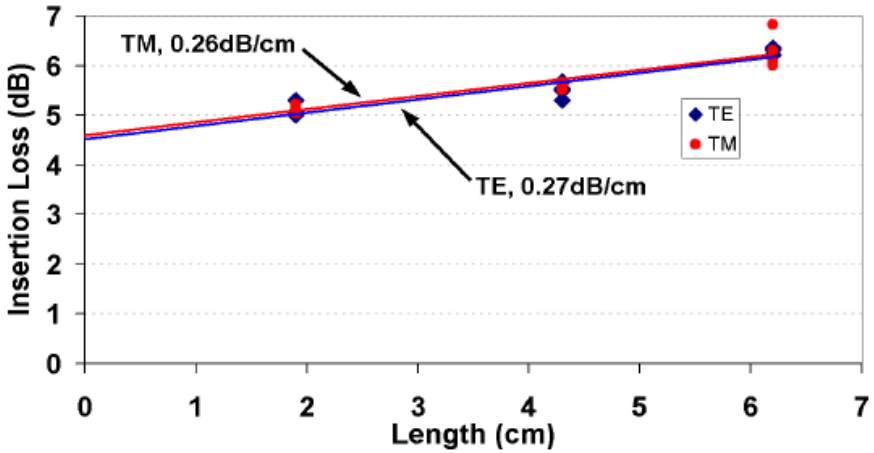

Fig. 4. Insertion loss of 3.3µm wide waveguides measured using cutback method.

Han et al, Opt. Express 18 (2010) 19286.

✓ Cutting and polishing bulk glass

- Sensor structure based on opto-electrophoretic detection
- GeAsTe glass having good mid IR transparence and electrical conductivity

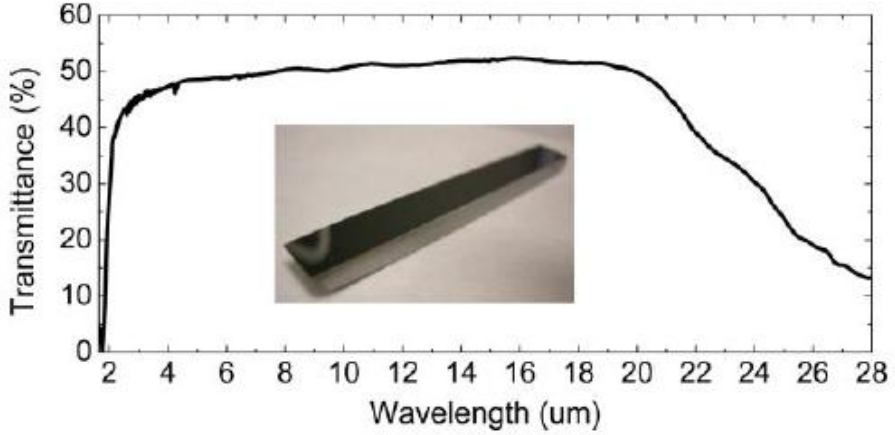

Fig. 1. Transmission spectrum of $Ge_{10}As_{15}Te_{75}$ glass, a 2 mm polished disk is used for the measurement; the inset is a photograph of the ATR plate made from $Ge_{10}As_{15}Te_{75}$ glass

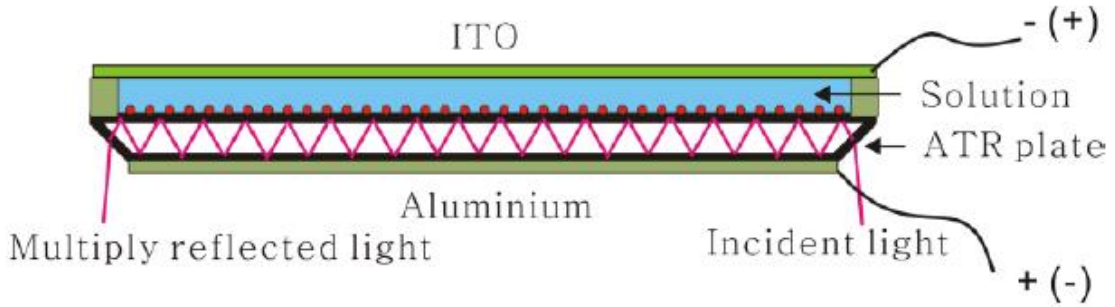

Fig. 2. (Color online) Schematic drawing of the electro-deposition device used for collection and analysis of charged biological molecules

Yang et al, Opt. Express 18 (2010) 26754.

✓ Solution processing

- ➢ As-S glass powder dispersed in propylamine

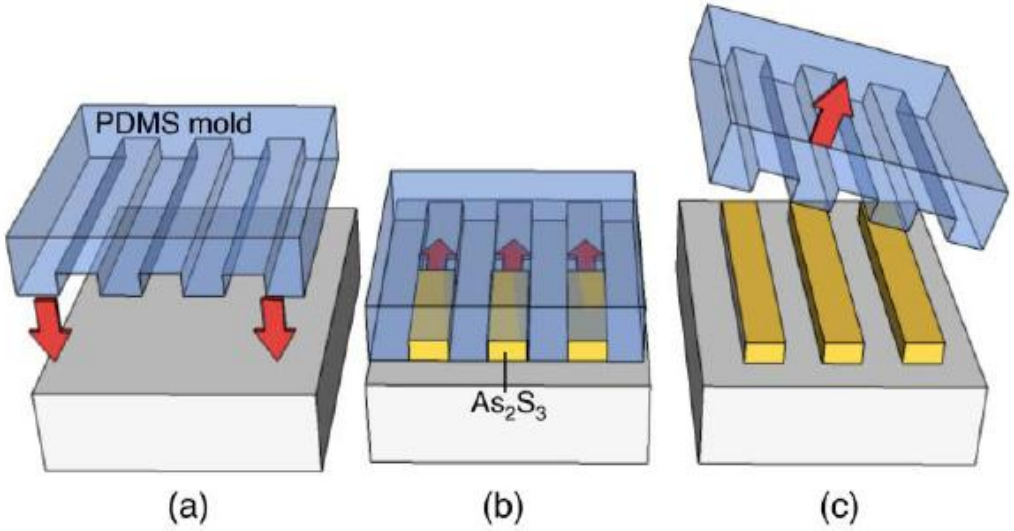

Fig. 2. Waveguides by MIMIC. (a) A PDMS mold with relief patterns is placed on a substrate to form micro-channels. (b) As_2S_3-propylamine solution (2g/10mL) is deposited at the channel inlets and flows into the channels by capillary action, at room temperature. (c) After the sample is baked (for 1 hr at 60°C and 2 hrs at 80°C, under vacuum) and the As_2S_3 solidified, the PDMS mold is peeled away.

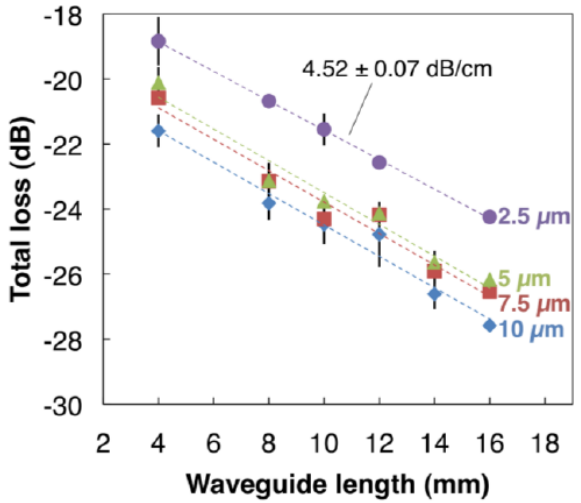

Fig. 6. Cut-back measurement. Losses of rib waveguides of varying width, with height = 4.5μm, on a $LiNbO_3$ substrate. The waveguides are aligned to and end-fired coupled to a QCL emitting at λ = 4.8μm. Each point represents averaged data from at least 5 different waveguides. Propagation loss of the 2.5μm wide waveguide is given.

Tsay et al, Opt. Express 18 (2010) 26744.

- ✓ Free falling and quenching
  - ➢ GaLaS glass doped with RE

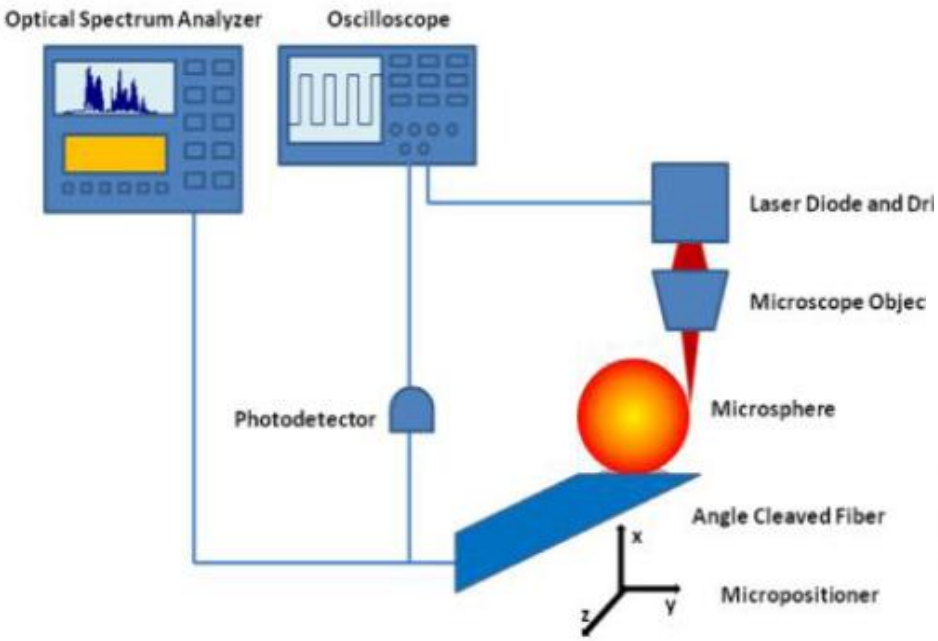

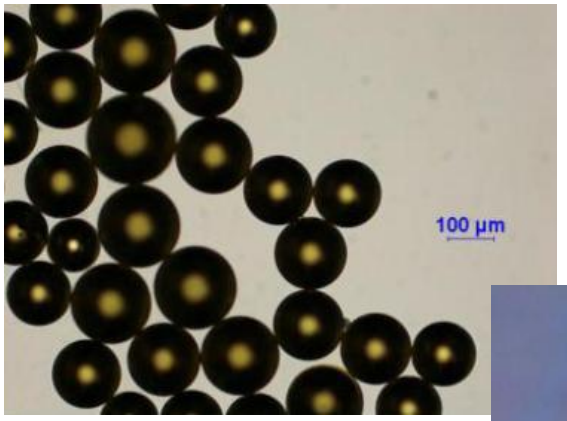

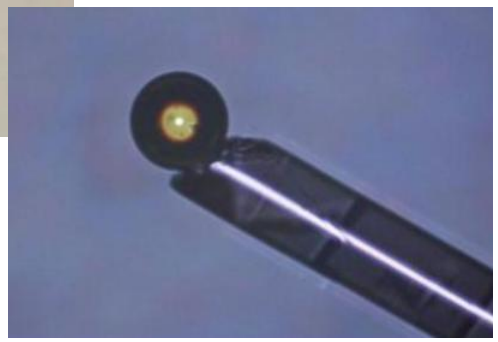

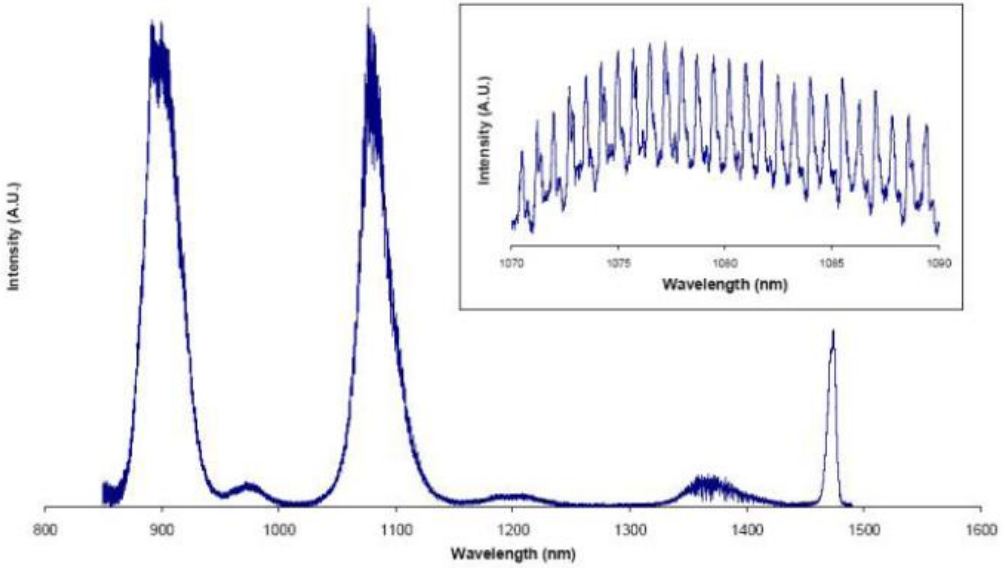

Fig. 4. Fluorescence spectrum from a GLS microsphere doped with 1.5 mol% Nd_2S_3. The inset shows the region between 1070 and 1090 nm, the region of interest in our laser experiments and the clear spectrum of whispering gallery modes supported by the sphere.

Elliott et al, Opt. Express 18 (2010) 26720.

Photonic crystal fiber

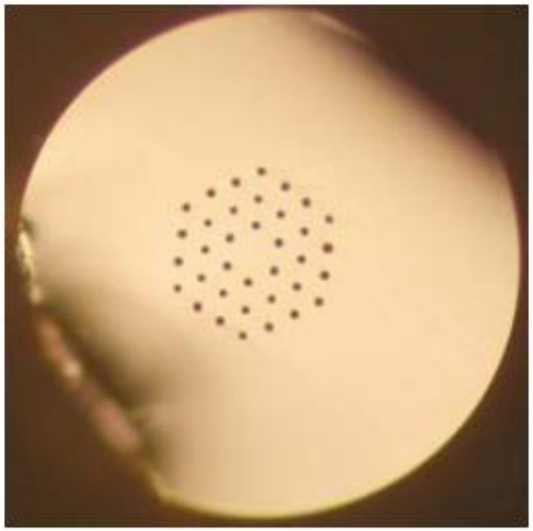

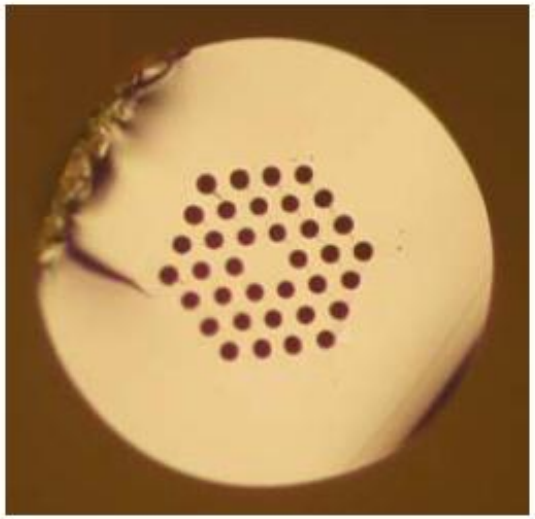

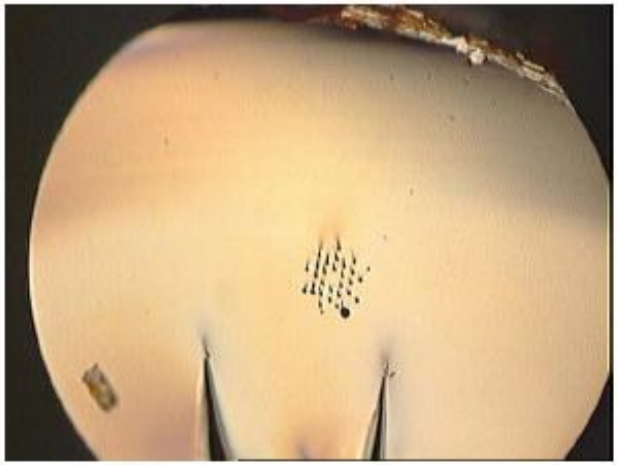

Figure 2 . Different geometries obtained on Chalcogenide holey fibers, (a) endlessy single mode fiber (Φ_{fiber} = 240 µm, A_{eff} = 150 µm^2, Λ = 14 µm, d/Λ=0,31), large mode effective area fiber (Φ_{fiber} = 400 µm, A_{eff} = 1000 µm^2, Λ = 28 µm, d/Λ=0,5), (c) small effective area fiber . (Φ_{fiber} = 80 µm, A_{eff} ~ 13 µm, Λ = 2,5 d/Λ=0,34).

Troles et al, ICTON 2007, pp. 297-300.

- ✓ Stack and draw method
  - Make glass rods with typical sizes around 18-cm length and around 12-mm outside diameter
  - Remelt to obtain the glass tube by centrifugation (tubes around 12-mm outside diameter about 5-mm inside diameter, and 12-cm length)
  - Draw drawn down to obtain capillaries of around 600-μm outside diameter
  - Stacked them in a hexagonal lattice around a central rod of the same diameter and placed into a larger jacket tube

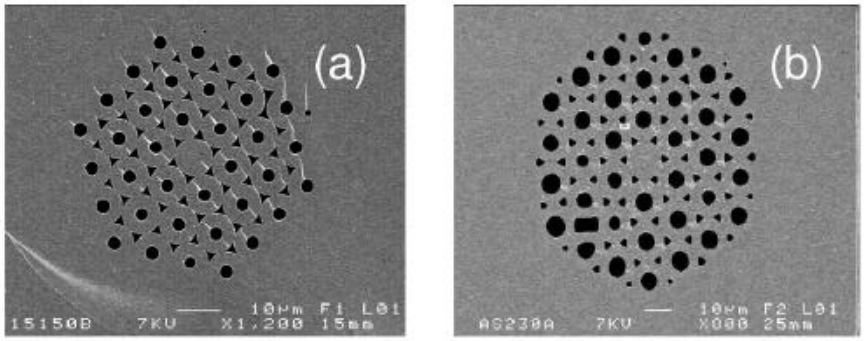

Fig. 1. (a) Cross section of GeSbS_2 PCF. (b) Cross section of AsSe PCF.

TABLE II
MEASURED OPTICAL PROPERTIES OF THE THREE MICROSTRUCTURED CHALCOGENIDE FIBERS

Parameter	*Fiber*		
	GeSbS_1	GeSbS_2	AsSe
Λ (μm)	9	13.25	7
d/Λ	0.31	0.31	0.42
A_{eff} (μm^2)	22	50	21
α (dB/m)	5	5.5	10
D ($ps/nm/km$)	-421	-406	-760
S ($ps/nm^2/km$)	0.9	1.1	2.7
DGD (ps/m)	5.5	0.8	1.24
Δn	$1.6\ 10^{-3}$	$2.4\ 10^{-4}$	$3.7\ 10^{-4}$
γ ($W^{-1}km^{-1}$)	517	227	2000
n_2 (m^2/W)	$2.8\ 10^{-18}$	$2.8\ 10^{-18}$	$1.1\ 10^{-17}$

Fatome et al, J. Lightwave Technol. 27 (2009) 1707.

✓ Casting method

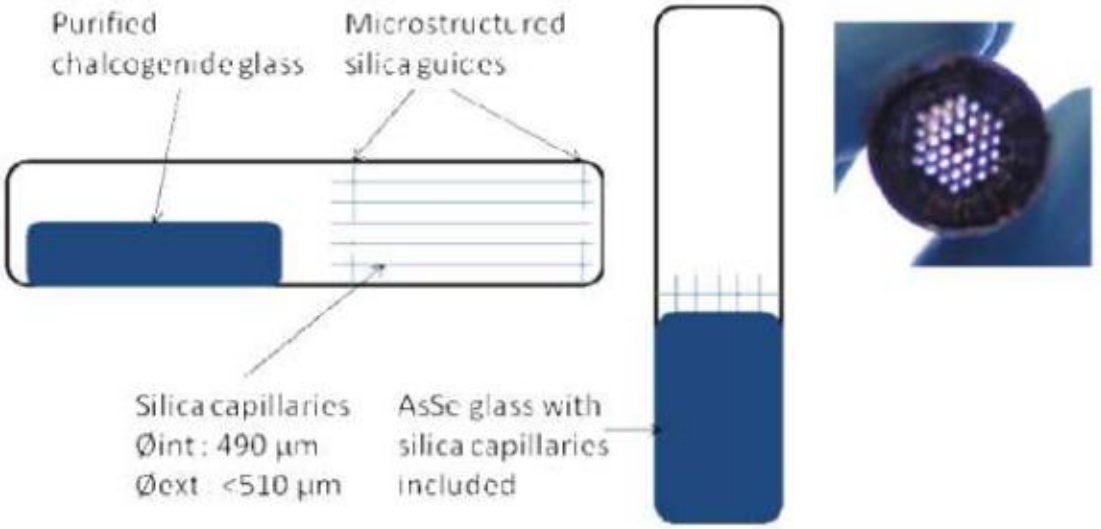

Fig. 1. Scheme of the silica mould. The glass is poured into the mould which is then removed by a HF treatment. The resulting preform is shown on the right picture.

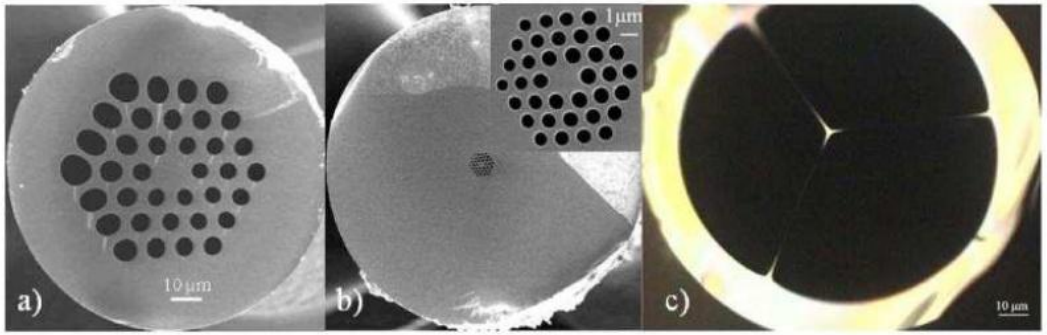

Fig. 2. a) SEM picture of a large core fiber. The core diameter is 13 µm. b) SEM picture of a small core fiber. The core diameter is around 2 µm. c) Optical microscopy picture of a suspended core fiber. The core diameter is 4 µm

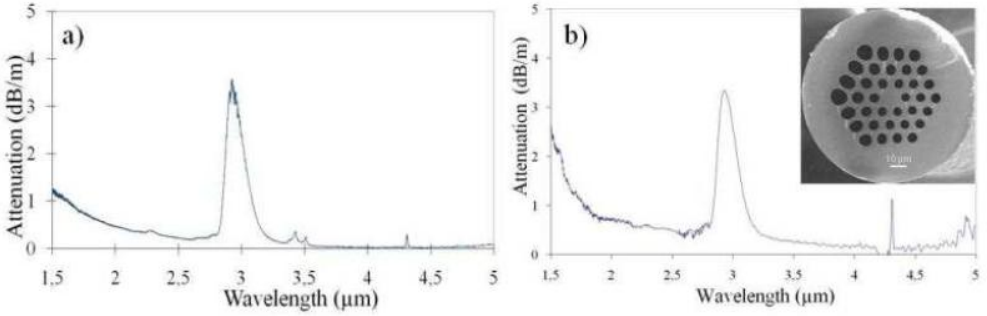

Fig. 3. a): Attenuation of the As_2Se_3 glass. b): Attenuation of the core of a multimode As_2Se_3 MOF.

Coulmobier et al, Optics Express 18 (2010) 9107.

2D photonic crystal

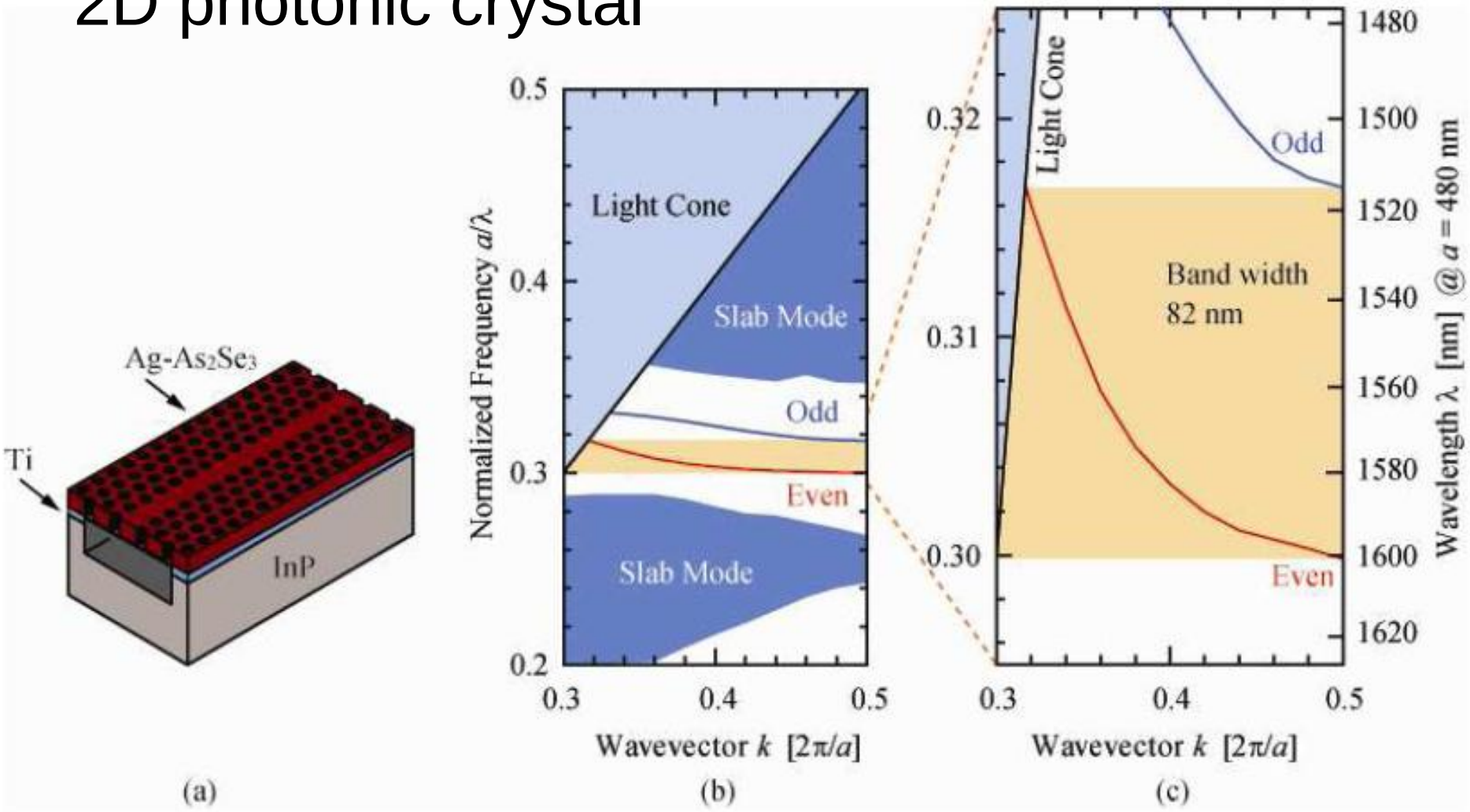

Fig. 1. (a) Schematic of chalcogenide glass photonic crystal waveguide. (b) Band diagram of Ag-As_2Se_3 photonic crystal waveguide. (c) Magnified figure of (b).

Suzuki et al, Optics Express 25 (2009) 22393.

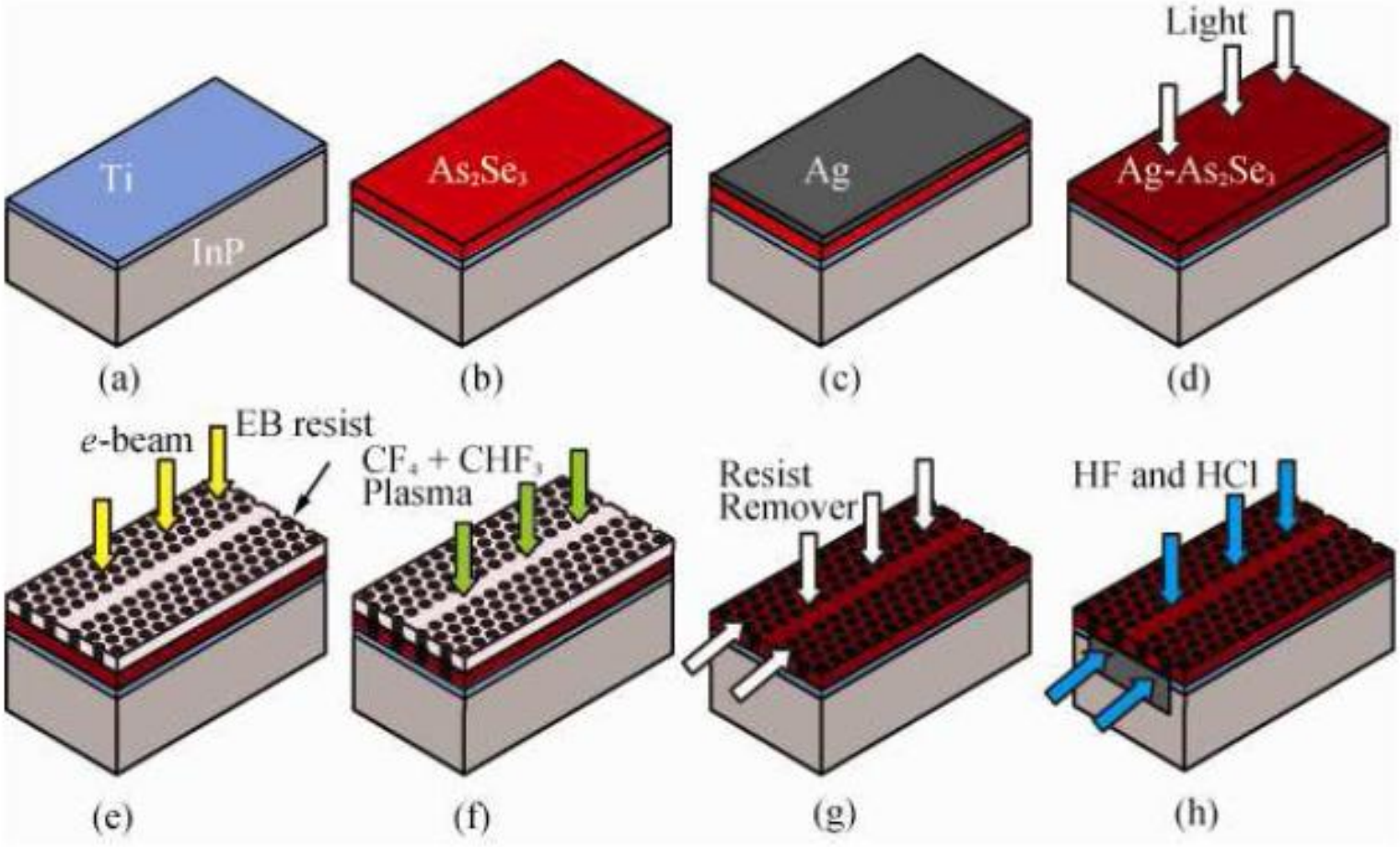

Fig. 2. Fabrication process of the Ag-As_2Se_3 chalcogenide glass photonic crystal waveguides. (a) Ti thermal evaporation. (b) As_2Se_3 thermal evaporation. (c) Ag thermal evaporation. (d) Photo-doping of Ag into As_2Se_3 using Halogen lamp. (e) EB writing of photonic crystal waveguides. (f) ICP etching using a CHF_3/CF_4 gas mixture. (g) EB resist removal using ZDMAC remover. (h) Wet-etching in HF and HCl solution.

Suzuki et al, Optics Express 25 (2009) 22393.

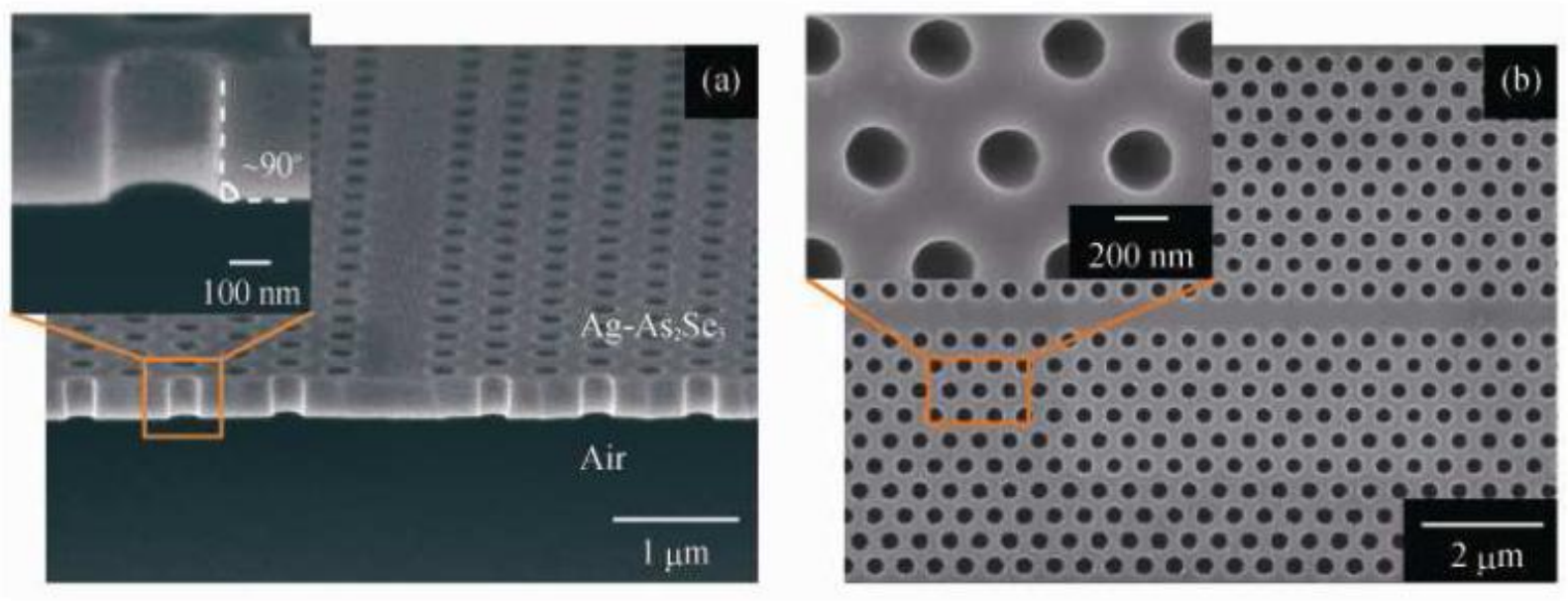

Fig. 3. SEM image of a fabricated Ag-As_2Se_3 photonic crystal waveguide. (a) Cross-sectional view. (b) Top view.

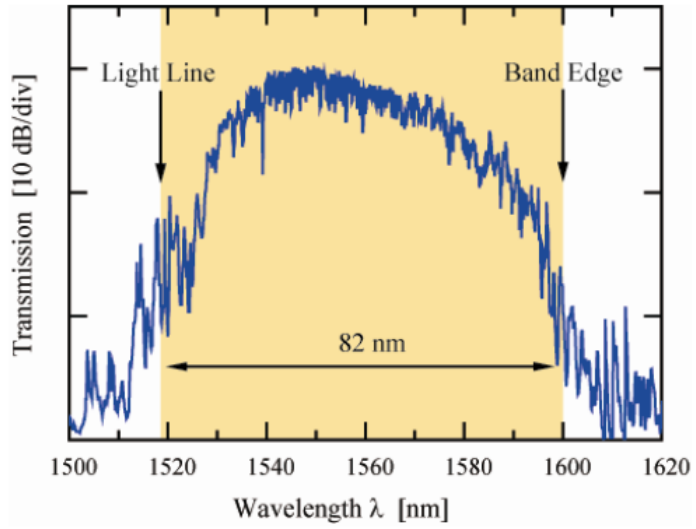

Fig. 4. Transmission spectrum of a fabricated chalcogenide glass photonic crystal waveguide.

Suzuki et al, Optics Express 25 (2009) 22393.

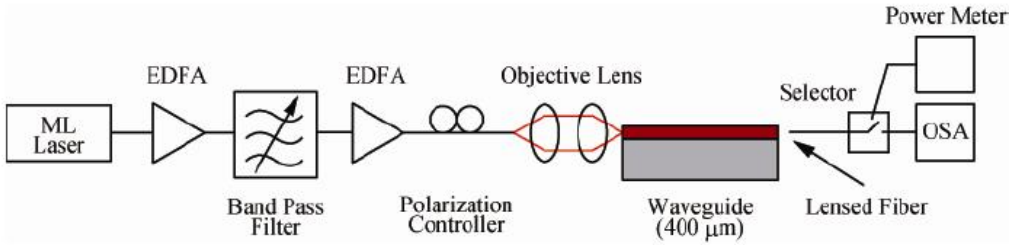

Fig. 5. Experimental setup for self-phase modulation.

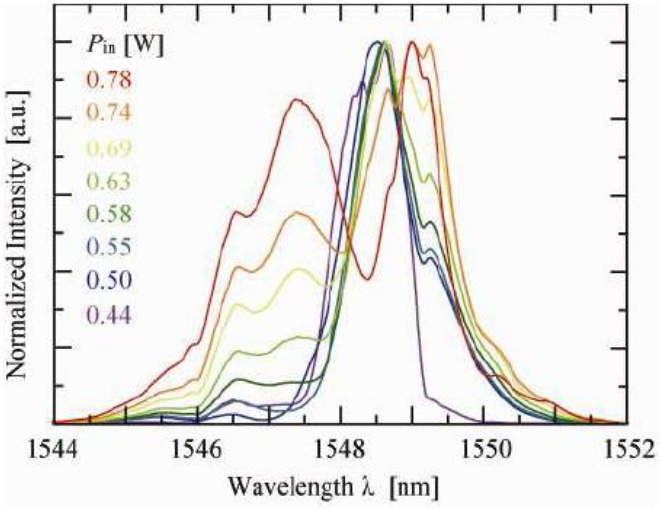

Fig. 6. Spectra of output pulse exhibiting SPM. Each spectrum is normalized to the peak magnitude

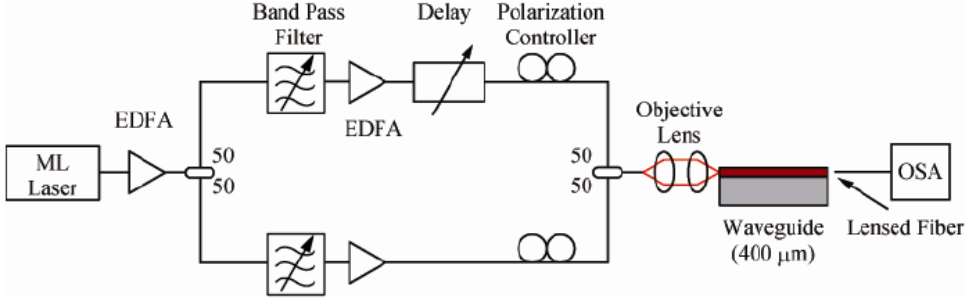

Fig. 8. Experimental setup for FWM.

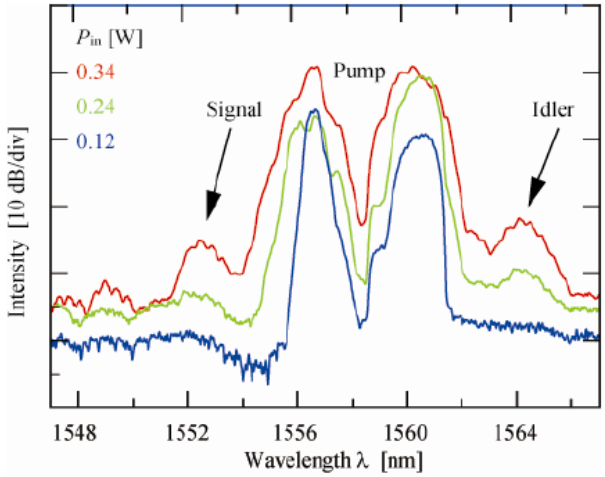

Fig. 9. Spectra of output pulse exhibiting FWM in Ag-As_2Se_3 PCW.

Suzuki et al, Optics Express 17 (2009) 22393.

✓ Anti-reflective surface structures

- ➢ Reduce Fresnel losses

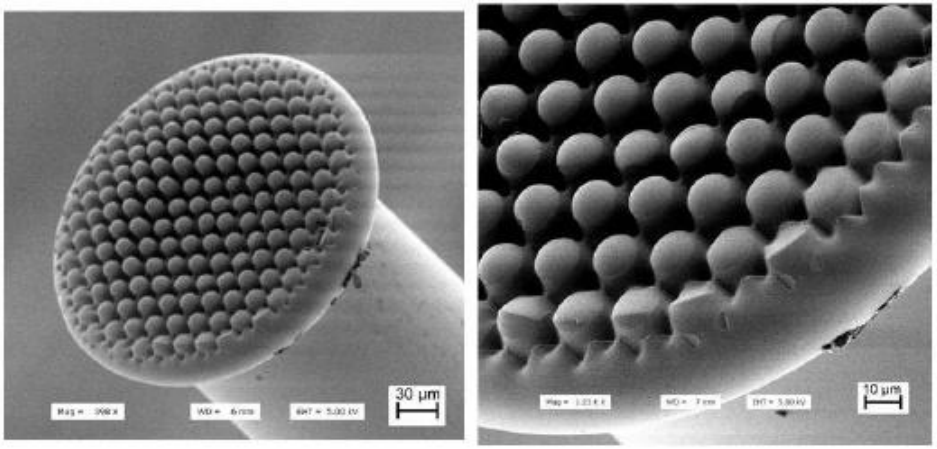

Fig. 3. SEM images of a stamped As_2S_3 fiber end - overview and detail. (30-µm and 10-µm markers, respectively).

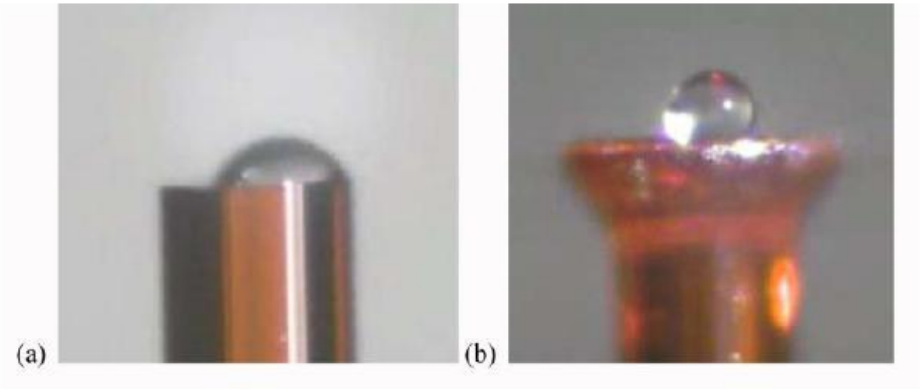

Fig. 8. Water droplet on surface of As_2S_3 glass fibers (a) cleaved surface (b) motheye-stamped surface.

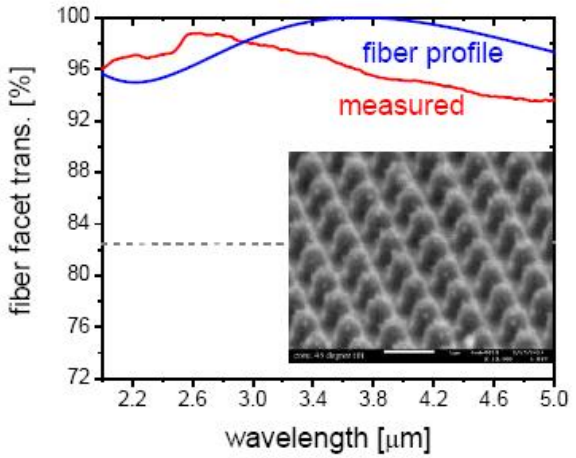

Fig. 9. Performance of stamped As_2S_3 fiber using shim 28B (feature height estimated at 849 nm). Inset shows patterned fiber end.

Sahghera et al, Optics Express 18 (2010) 26760.